CYLINDRICAL OBSTACLE EFFECT ON CONVECTION INSIDE AN INCLINED ENCLOSURE FILLED WITH A NANOFLUID

UDC:532:536.2-026.71
Original scientific paper https://doi.org/10.46793/aeletters.2024.9.1.3

Nadia Kaddouri[1*], Sahraoui Kherris[2], Kouider Mostefa[2], Said Mekroussi[1], Momen SM Saleh[3], Djallel Zebbar[2]

[1]Research Laboratory of Industrial Technologies, Faculty of Applied Sciences, University of Tiaret, B.P. 78 Zaâroura 14000 Tiaret, Algeria
[2]Laboratory of Mechanical Engineering, Materials and Structures, Tissemsilt University, Benhamouda B.P. 182, 38010 Tissemsilt, Algeria
[3]Laboratory of Materials and Energy Engineering (LGEM), University of Mohamed Khider Biskra, Algeria

Abstract:
This study investigated the impact of a cylindrical obstacle on convection in an inclined square cavity filled with water-Al_2O_3 nanofluid. Using the finite volume method, the problem was resolved by having the inner cylinder rotate adiabatically while other walls were thermally insulated. Additionally, the bottom wall was hotter than the top. The study examined the effects of cylindrical obstacle radius ($0.1 \leq R \leq 0.2$), rotation speed ($-500 \leq \Omega \leq 500$), Richardson number ($0.01 \leq Ri \leq 100$), volumetric nanoparticle fraction (0.02), and Grashof number ($Gr = 10^4$) on heat transfer rate or Nusselt number. The results were compared with previous literature, and the influence of the cylindrical obstacle rotational speed on convection flow was evaluated. An increase in the counterclockwise angular rotating speed resulted in higher nanofluid flux. The heat transmission coefficient increased as the Richardson number decreased. The use of nanofluid in the enclosure increased the coefficient of heat flow through mixed convection. Finally, the study showed that the convection heat exchange is enhanced with the increase in the radius. Moreover, an enhancement of the Nusselt number around 46% was reported for the cylinder, under Gr=10000, Ø=0.02, γ=45° and Ri= 10.

ARTICLE HISTORY
Received: 25 December 2023
Revised: 24 February 2024
Accepted: 8 March 2024
Published: 31 March 2024

KEYWORDS
Mixed convection, Nanofluids, Rotating Cylindrical obstacle, Heat exchange, Water-Al_2O_3, Radius, Rotational speed

1. INTRODUCTION

The mixed convection flow in a cavity filled with a nanofluid was the subject of numerous studies by researchers. Several engineering applications for mixed convection in cavities include cooling electronic components, food drying, and nuclear reactors [1]. An essential liquid with suspended metallic or non-metallic nanoparticles is called a nanofluid. Water, oil, and ethylene glycol are often studied fluids for various industrial uses, such as cooling and heating systems [2]. Soomro et al. [3] have looked into the thermal efficiency of magnetohydrodynamic mixed convection inside the cover-driven triangle cavity with a circular obstacle. Pal et al. [4], examined the impact of a thick corrugated wall on the heat transfer of mixed convection filled with a copper-water nanofluid in a square cavity. Muthtamilselvan et al. [5] achieved a numerical analysis of a mixed convection flow in a square enclosure with a lid containing a Cu-water nanofluid in addition to internal heat generation. According to Abu-Nada et al. [6], the concentric rings of natural convection were filled with a nanofluid in this simulation. The later study took into account four different kinds of nanoparticles. Among others, Yousefzadeh et al. [7], carried out an analysis using numerical methods of the behavior of

*CONTACT: Nadia Kaddouri, e-mail: nadia.kaddouri@univ-tiaret.dz

mixed convection filled with a nanofluid inside a cavity with a hot obstacle. Shekaramiz et al. [8] conducted a study of the natural convection of water-Fe_3O_4 in the wavy triangular with equilateral sides and examined numerically with two geometries (n = 3 and 6) for various undulations numbers. Incompressible mixed convection with a nanofluid inside of a vented cavity with a cylindrical obstruction was studied by Jasim et al. [9]. Al‑Kouz et al. [10] investigated the flow of mixed convection in the presence of a solid cylinder inside a square cavity filled with water-alumina nanofluid and having vertical walls with corrugations. Rahmati et al. [11] employed the lattice Boltzmann approach to investigate the natural convection of water-TiO_2 in a square cavity in the presence of a heated obstruction. Sivanandam et al. [12] have investigated the effects of entropy production and the movable walls' orientation on the nanofluid's mixed convective flow and the energy transfer of the nanoliquids. Selimefendigil et al. [13], the mixed convection of an elliptical obstacle inside a square cavity filled with nanofluid might be studied using the finite element method and the optimization solver COBYLA. Mixed convection has been investigated and reported by Azizul et al. [14], in a heated cavity with waves that contain nanofluids and a solid inner body. Maiga et al. [15], laminar forced convection flows with a nanofluid within were investigated in a tube with a circular section to maximize heat transmission in a rectangle with four walls pushed by a cover. Ambethkar et al. [16] did a numerical analysis using nanotechnology of how moving walls affect fluid flow to increase heat transmission. Al-asadi et al. [17], study the flows of nanofluids with mixed convection in an inclined circular tube for improved heat transfer by nanotechnology. Many researchers have researched the effects of various parameters in their work, including the Ra number, Volume percentage of nanofluid, and Ri number. From their findings, it has been found that the Ra number and Ri number have considerable value in the Nu number [18-20].

The application of sinusoidal heating in cavities filled with nanofluids has been extensively studied for its crucial role in heat transfer, but there are still some limitations in this area. The rapid development of the CPU and GPU that the world has witnessed has created many problems that cannot be overlooked. The most important of these major problems is high heat generation, which in turn slows down performance and reduces lifespan. It has become essential to eliminate or reduce heat using a variety of different cooling technologies; this is to preserve performance and lifespan.

This study aims to overcome these limitations using a new non-uniform temperature distribution, which has widespread applications in heating and cooling equipment, solar energy, drying equipment, and nuclear reactors. The research investigates the mixed convection flux of Al_2O_3-water nanofluid in a double-lid inclined square cavity with cylindrical obstacles. The study aims to analyze the isotherms and streamlines of heat flow using dimensionless variables such as the Richardson number, angular rotational velocity, and radius of a rotating cylinder.

2. MATHEMATIC AND MODELING FORMULATION

This study investigates mixed heat transfer conditions in a two-dimensional flow within an inclined square cavity of height and width L, involving a spinning cylinder with a radius of R (see Fig. 1). The flow is incompressible, laminar, stagnant, and convective. The cylinder and vertical walls are adiabatic; the cylinder rotates in clockwise and counter-clockwise directions, and the left and right walls move in opposite directions. The lower wall has a higher sinusoidal temperature than the top wall. The Boussinesq approximation is considered appropriate, and the Navier-Stokes equations are used, considering above assumptions [21].

The thermophysical properties of nanofluid are shown in Table 1.

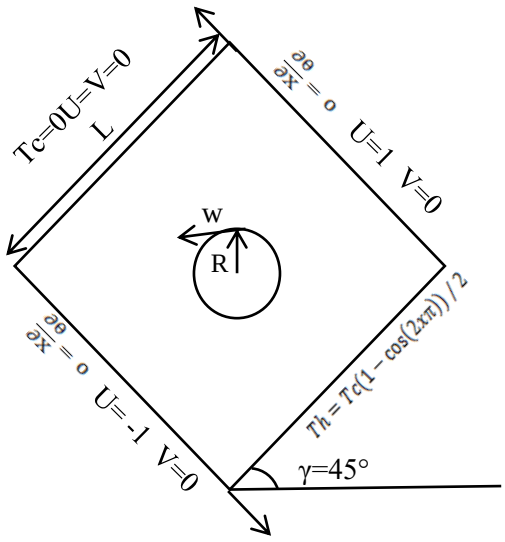

Fig. 1. Dimensions of the cavity and its boundaries

In Fig. 2. The networks used in the current simulation are shown.

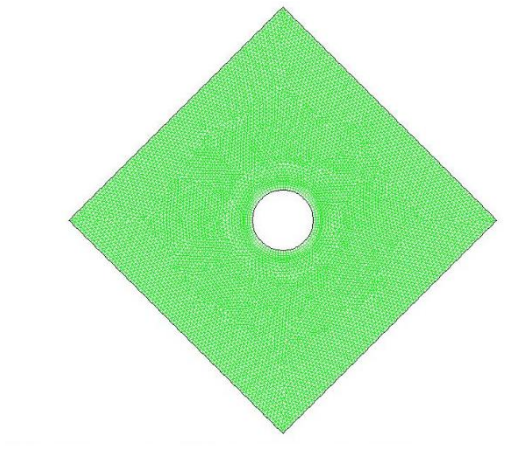

Fig. 2. The meshes employed in the current simulation

Table 1. Represents the thermophysical properties of nanofluid [1]

Property	Water	Al_2O_3
Cp (J/kg K)	4179	765
ρ (kg/m³)	997.1	3970
K (W /m K)	0.613	40
β×10⁻⁵(1/K)	21	0.85
μ×10⁻⁴(Kg/m·s)	8.9	_

These are the equations dimensionless forms [22]:

$$\frac{\partial U}{\partial X}+\frac{\partial V}{\partial Y}=0 \quad (1)$$

$$U\frac{\partial U}{\partial X}+V\frac{\partial U}{\partial Y}=-\frac{\partial P}{\partial X}+\frac{\upsilon_{nf}}{\upsilon_f}\frac{1}{\mathrm{Re}}.\nabla^2 U+\frac{Ri}{\mathrm{Pr}}.\frac{\beta_{nf}}{\beta_f}\theta\sin\gamma \quad (2)$$

$$U\frac{\partial V}{\partial X}+V\frac{\partial V}{\partial Y}=-\frac{\partial P}{\partial Y}+\frac{\upsilon_{nf}}{\upsilon_f}\frac{1}{\mathrm{Re}}.\nabla^2 V+\frac{Ri}{\mathrm{Pr}}.\frac{\beta_{nf}}{\beta_f}\theta\cos\gamma \quad (3)$$

$$U\frac{\partial\theta}{\partial X}+V\frac{\partial\theta}{\partial Y}=\frac{\alpha_{nf}}{\alpha_f}\nabla^2\theta \quad (4)$$

where are:

U, V - dimensionless of velocity component;
X, Y - dimensionless of Cartesian;
P - dimensionless pressure;
υ -Kinematic viscosity, (m^2/s);
Re - Reynolds number;
Ri - Richardson number;
Pr - Prandtl number;
β - thermal expansion coefficient, (1/K);
ϑ - dimensionless temperature;
γ - Inclination angle of a cavity, (°);
α - Thermal diffusivity, (m^2/s).

The reduced variables used to dimension equations (1-4) are those produced by the following expressions [23]:

$$X=\frac{x}{L},Y=\frac{y}{L},U=\frac{u}{U_0},V=\frac{v}{U_0}, \quad (5)$$

$$p=\frac{p}{\rho_{nf}U_0^2},\theta=\frac{T-T_C}{T_h-T_C},\Omega=\frac{\omega L^2}{\alpha_{nf}} \quad (6)$$

where are:

x, y - Cartesian coordinates, (m);
u, v - components of velocity, (m/s);
p - pressure, (N/m^2);
ρ - density, (kg/m^3);
T - temperature, (K);
Ω - dimensionless angular rotational velocity;
ω - angular rotational velocity, (rad/s);
L - cavity height/width, (m);
C - cold;
h - hot.

The dimensionless parameters are expressed as [24]:

$$\mathrm{Re}=\frac{\rho_f U_0 L}{\mu_f},\ Ri=\frac{g\beta_f\Delta TL}{U_0^2}=\frac{Gr}{\mathrm{Re}^2}, \quad (7)$$

$$\mathrm{Pr}=\frac{\upsilon_f}{\alpha_f},\ Gr=\frac{g\beta\Delta TL^3}{\upsilon^2} \quad (8)$$

where are:

Gr- Grashof number;
μ - dynamic viscosity, (kg/ms);
g - gravitational acceleration, (m/s^2).

The cavity current geometry has the following boundary conditions:

X = 0, $0\le Y\le 1$, U = 0, V = -1, $\frac{\partial\theta}{\partial X}=0$

X = 1, $0\le Y\le 1$, U = 0, V = -1, $\frac{\partial\theta}{\partial X}=0$

Y = 0, $0\le X\le 1$, U = 0, V = 0,

$\theta=\left(1-\cos(2x\pi)\right)/2$

Y = 0, $0\le X\le 1$, U = 0, V = 0, $\theta=0$

On the lower wall are the regional and typical Nusselt numbers, which are [25]:

$$Nu=-\left(\frac{k_{nf}}{k_f}\right)\frac{\partial\theta}{\partial y} \quad (9)$$

$$Nu_{avg}=\int_0^1 Nu(x)dx \quad (10)$$

where are:

Nu - Nusselt number;

k -thermal conductivity, (W/m K);

avg - average.

The following equations are used to calculate the mixture density (ρ), specific heat capacity (Cp), and thermal expansion coefficient (β) of the nanofluid [26]:

$$\rho_{nf} = (1-\phi)\rho_f + \phi\rho_S \quad (11)$$

$$(\rho C_p)_{nf} = (1-\phi)(\rho C_p)_f + \phi(\rho C_p)_S \quad (12)$$

$$(\rho\beta)_{nf} = (1-\phi)(\rho\beta)_f + \phi(\rho\beta)_S \quad (13)$$

where are:

ϕ -volume fraction of nanofluid;

C_p - specific heat capacity (J/kg K);

nf -nanofluids;

f- fluid;

s - solid.

Brinkman's relationship was used to determine the viscosity of the nanofluid [27]:

$$\mu_{nf} = \frac{\mu_f}{(1-\phi)^{2.5}} \quad (14)$$

The Maxwell model has been used to calculate the thermal conductivity of the nanofluid model [28]:

$$\frac{k_{nf}}{k_f} = \frac{(k_S + 2k_f) - 2\phi(k_f - k_S)}{(k_f + 2k_S) + 2\phi(k_f - k_S)} \quad (15)$$

3. NUMERICAL APPROACH

The pressure and velocity were calculated from the momentum and energy equations using a SIMPLE algorithm using the finite volume technique [29] using fluent software. The fluid flow field and convection properties were simulated using Fluent. The Quick diagram defines the convective conditions of Navier Stokes equations using a central feature element. Table 2 shows the Nusselt number for testing the uniform grid at Re 500 and Pr = 0.71 for several systems and compared with [30], where the grid 81X81 was chosen in the current study. A numerical procedure is validated for a uniform grid (81 × 81) of the average Nusselt number for 1 < Re < 1000 and Gr = 100 is validated and compared with the numerical results from theChamkha and Abu-Nada [2], as shown in Table 3.

Table2. The effect of the meshon average Nusselt number

Grid	42×42	60×60	81×81	100×100	Ref.[30]
Re=500 Pr=0.71	5.145	5.291	5.357	5.386	5.168

Table 3. Comparing the average Nusselt number calculated in this study with past works by Chamkha and Abu-Nada [2]

Re	Present work (81×81)	Ref.[2]	Ref.[31]	Ref.[32]	Ref.[33]	Ref. [34]	Ref.[35]	Ref.[36]	ε
1	0.992569	1.010134	1.00033	-	-	-	-	-	0.01756
100	2.022933	2.090837	2.03116	2.10	1.985	2.02	-	2.01	0.06790
400	4.049844	4.162057	4.02462	3.85	3.8785	4.01	4.05	3.91	0.11221
500	4.558188	4.663689	4.52671	-	-	-	-	-	0.10550
1000	6.527703	6.551615	6.48423	6.33	6.345	6.42	6.55	6.33	0.02391

The current numerical solution is valid by comparing the contours distribution for Re = 500, Ri = 0.4, and Pr = 1 with the results of M.K. Moallemi and K.S. Jang [30], as shown in Figs. 3 and 4. A good agreement is thus obtained. The absolute error between the values obtained in the current study and the previous study was calculated as equal to 0.0983.

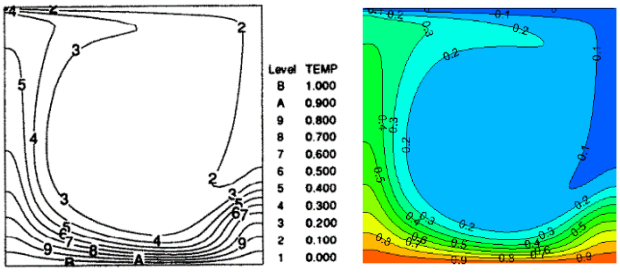

a) b)

Fig. 3. Isotherms for Re = 500 and Pr = 1: a) Results of Moallemi and Jang [30], b) Current study

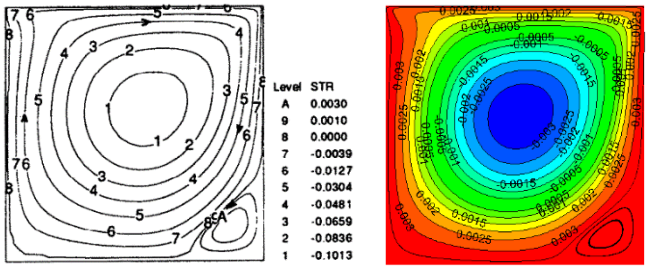

a) b)

Fig. 4. Streamline for Re = 500 and Pr = 1: a) Results of Moallemi and Jang [30], b) Current study

4. RESULTS AND DISCUSSION

Studying the effect of rotating cylinder adiabatic on the heat flow was the primary goal of this work by mixed convection in an inclined square cavity with double lid-driven walls filled with water–Al_2O_3 nanofluids for Ri = 0.01 to 100, Gr=10000, R = 0.1 to 0.2, Ω = -500 to 500 and ϕ = 0.02. The bottom wall has a hotter temperature than the top wall. Also, the other wall was kept thermally isolated and moving in the opposite direction.

Figs. (5, 6, 9, and 10) display the streamlines and isotherms for the mentioned cases at Gr=10000 and ϕ=0.02, γ =90° and R=0.1, 0.2 for various Richardson numbers and cylinder angular velocity. As seen in Figs. 5 and 6, at Ω=0, the heat transferred from the lower horizontal wall to the left vertical wall only increases the Richardson number by (0.01 to 100), with an angular rotation speed in counter-clockwise still increasing at Ω= -500, thermal performance increases. Heat and nanofluid travel down to the left of the cavity since the vertical walls' movement is in the opposite direction. More isothermal lines travel to the left wall as a result of the cylinders' negative rotating speed.

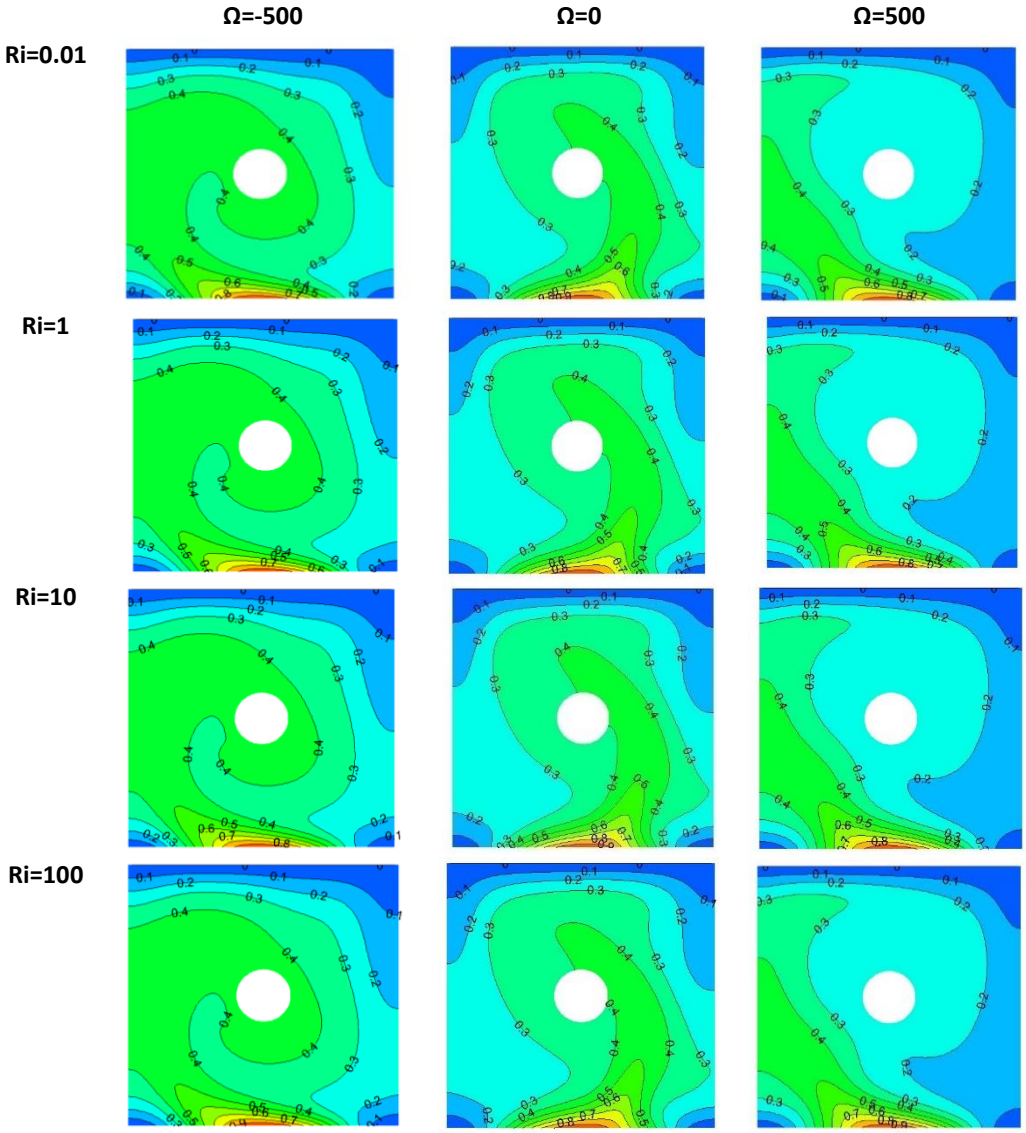

Fig. 5. Isotherms for 0.01 ≤ Ri ≤ 100,-500 ≤ Ω ≤ 500, R= 0.1 and γ=90°

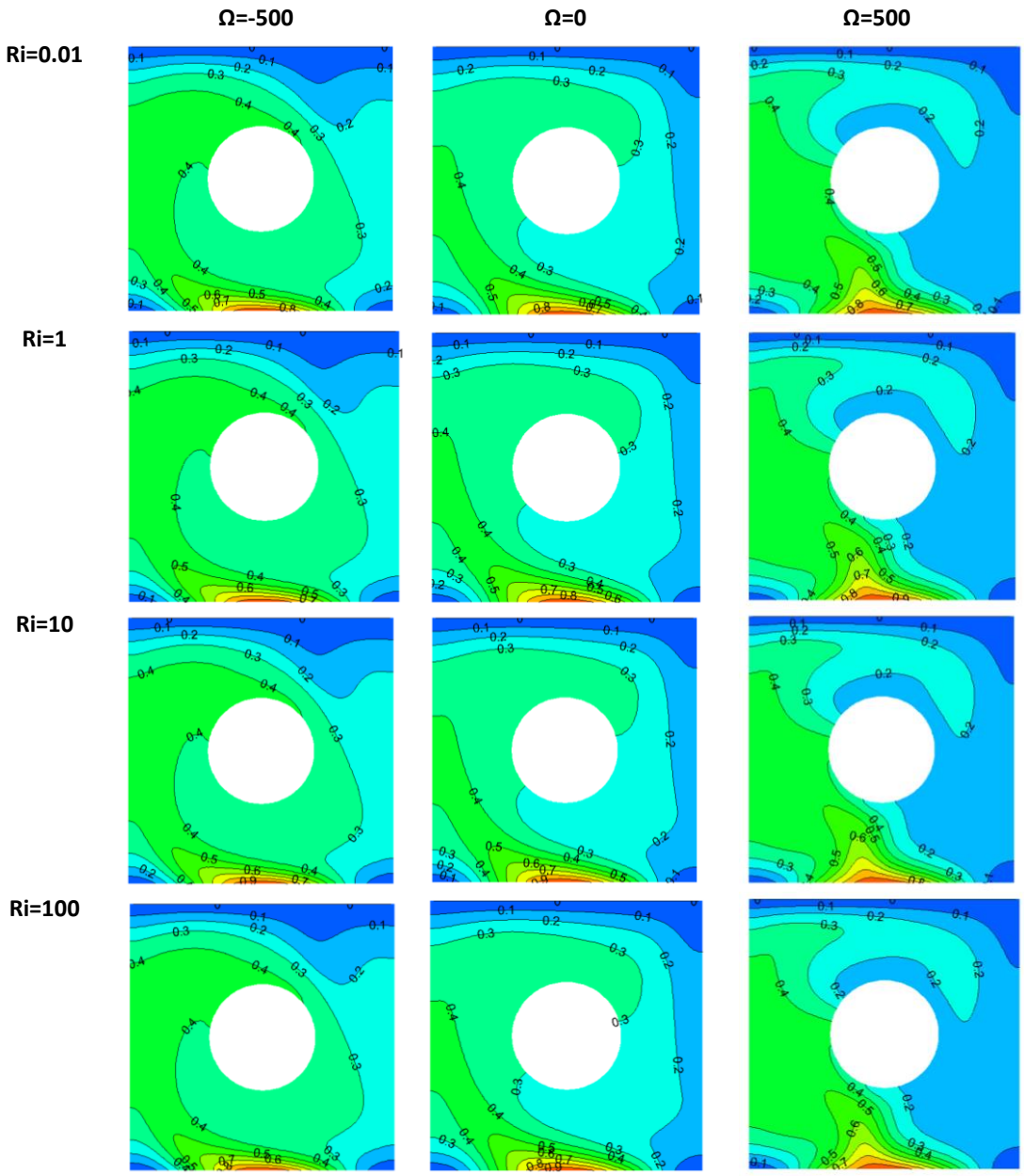

Fig. 6. Isotherms for 0.01 ≤ Ri ≤ 100,-500 ≤ Ω ≤ 500, R = 0.2 and γ=90°

The contours in Figs. 9 and 10 demonstrate that as counter-clockwise angular rotational velocity increases, thicker streamlines and larger vortices are produced at Ω= -500. An increase increases the influence of convective flow caused by the lid; in this instance, the double-lid effect is more evident. The movement of the fluid is faster near the cylinder when the cylinder rotation speed is in the clockwise and counterclockwise direction and becomes weaker when the cylinder is stationary Ω=0. Since the fluid flow is near the cylinders due to the rotational force induced by the shear stress, the two cylinders' respective diameters of 0.1 and 0.2 impact the fluid flow.

The Figs. (7, 8, 11 and 12) show streamlines and isotherms for different -500 ≤ Ω ≤ 500and 0.01 ≤ Ri ≤ 100 for the instances discussed at Gr=10000, ϕ=0.02, γ=90° and R=0.1, 0.2. From Figs. 7 and 8, for the case Ri = 10, 100 and Ω= -500, the heat increases in the lower wall and is slightly transferred to the right wall. The heat flow by convection was boosted by increasing the Richardson number and counterclockwise angular rotational speed. The cylinder rotation alters the distribution of isotherms and the fluid flow in the cavity.

The cylinder rotation causes the streamline modifications to occur near the cavity center. Ri = 10 and 100 in Figs. (11 and 12) results in stronger vortices. As the Richardson number rose, more streamlines were close to the hollow and lid walls. A significant rotating vortex may typically be seen. So, there has been a rise in streamlining overall.

Therefore, the revolving cylinder speed alters the flow pattern and raises sheer force. Increase the impact of the heat flow that the cover produces. The double-hedging flow effect is more pronounced in this situation.

When the cylinders rotate clockwise Ω=500, mixed convection currents are inhibited, while the opposite is true for counter-clockwise rotation Ω=-500. Compared to a stationary cylinder Ω=0, rotating the cylinder introduces additional momentum exchange, leading to changes in fluid flow and isotherm distribution within the cavity.

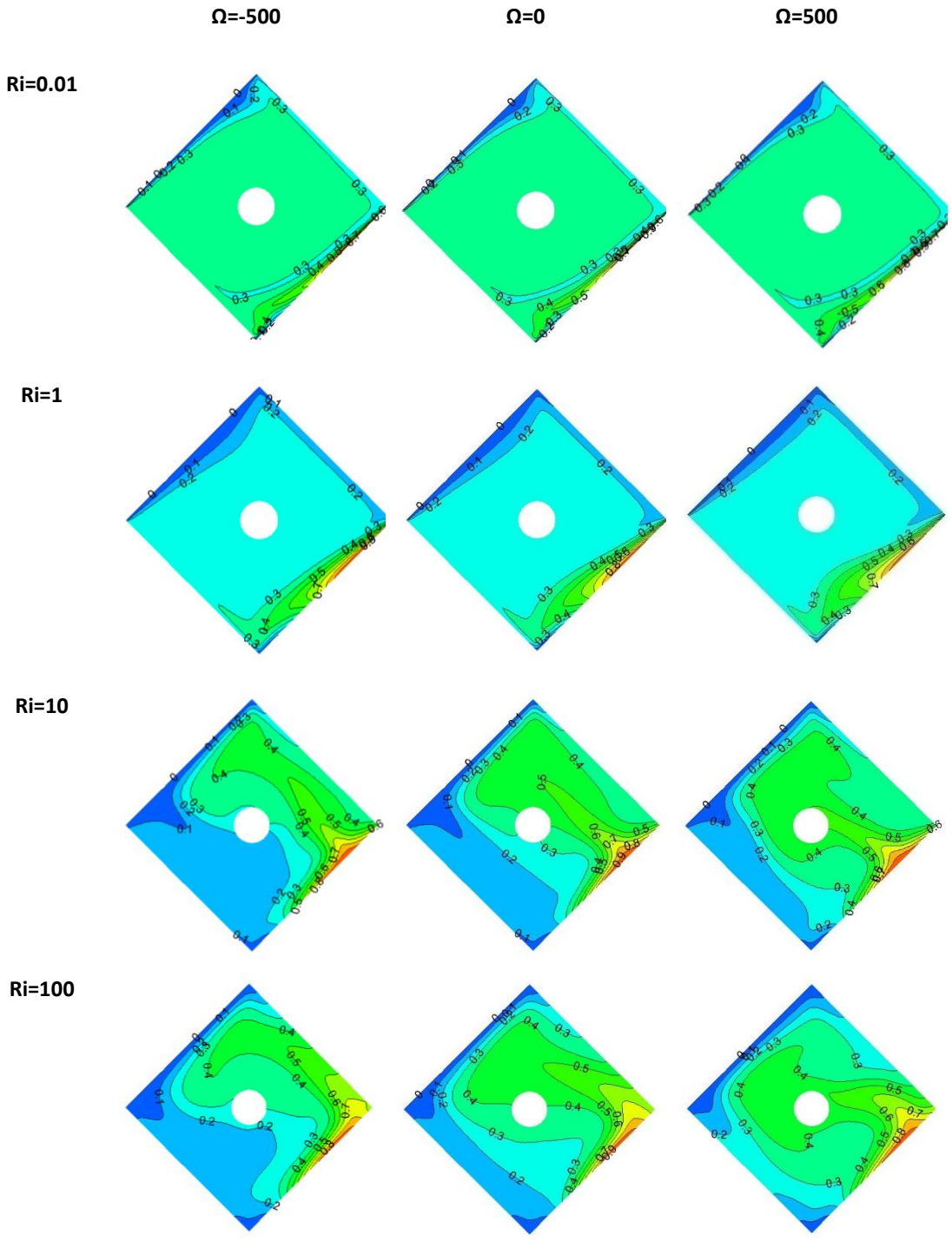

Fig. 7. Isotherms for 0.01 ≤ Ri ≤ 100,-500 ≤ Ω ≤ 500, R =0.1 andγ =45°

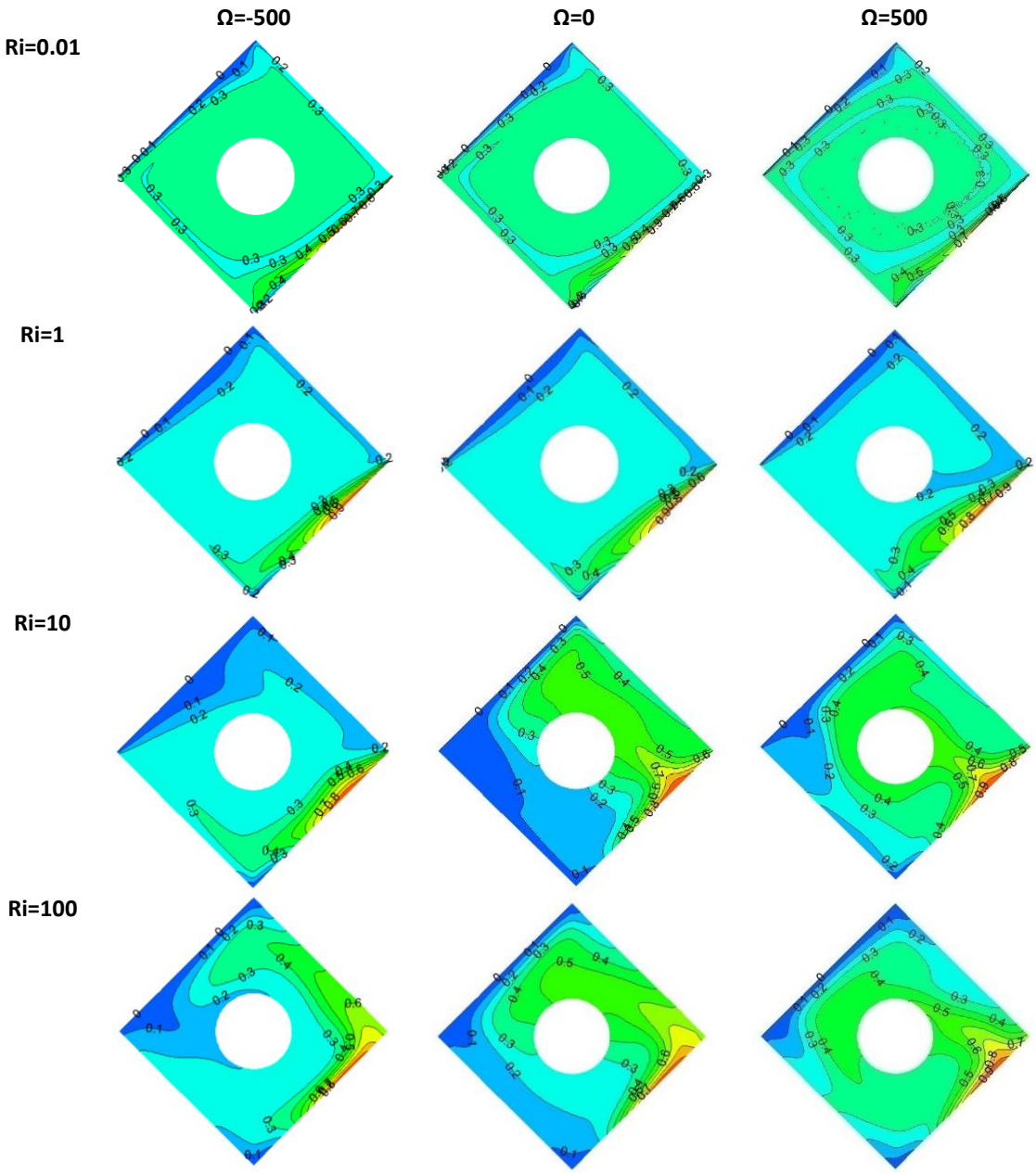

Fig. 8. Isotherms for 0.01 ≤ Ri ≤ 100, -500 ≤ Ω ≤ 500, R = 0.2 and γ=45°

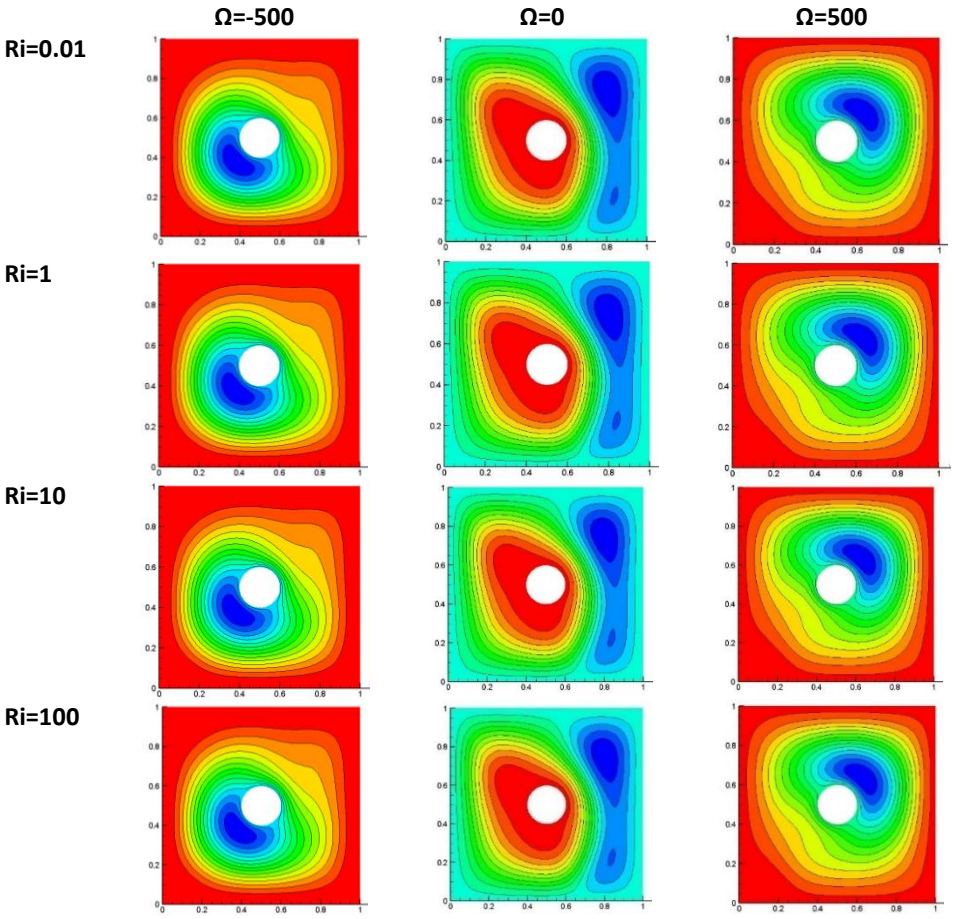

Fig. 9. Streamlines for 0.01 ≤ Ri ≤ 100, -500 ≤ Ω ≤ 500, 0.1, R =0.1 and γ=90°

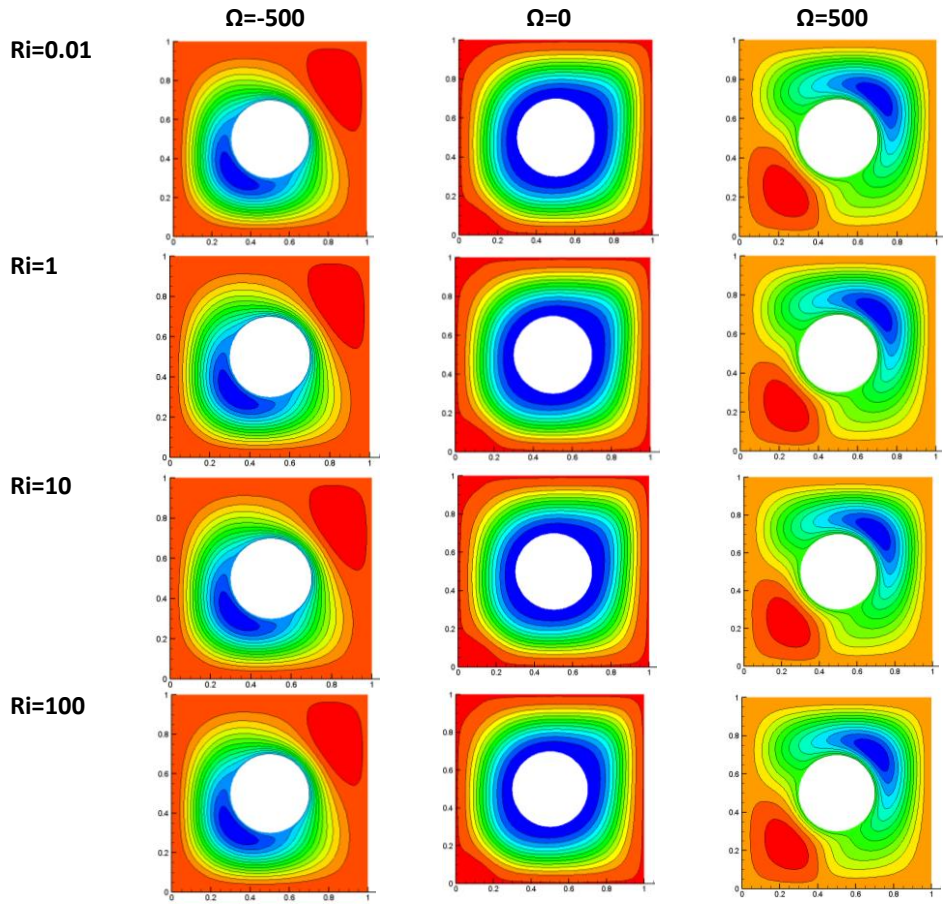

Fig. 10. Streamlines for 0.01 ≤ Ri ≤ 100, -500 ≤ Ω ≤ 500, R = 0.2 and γ =90°

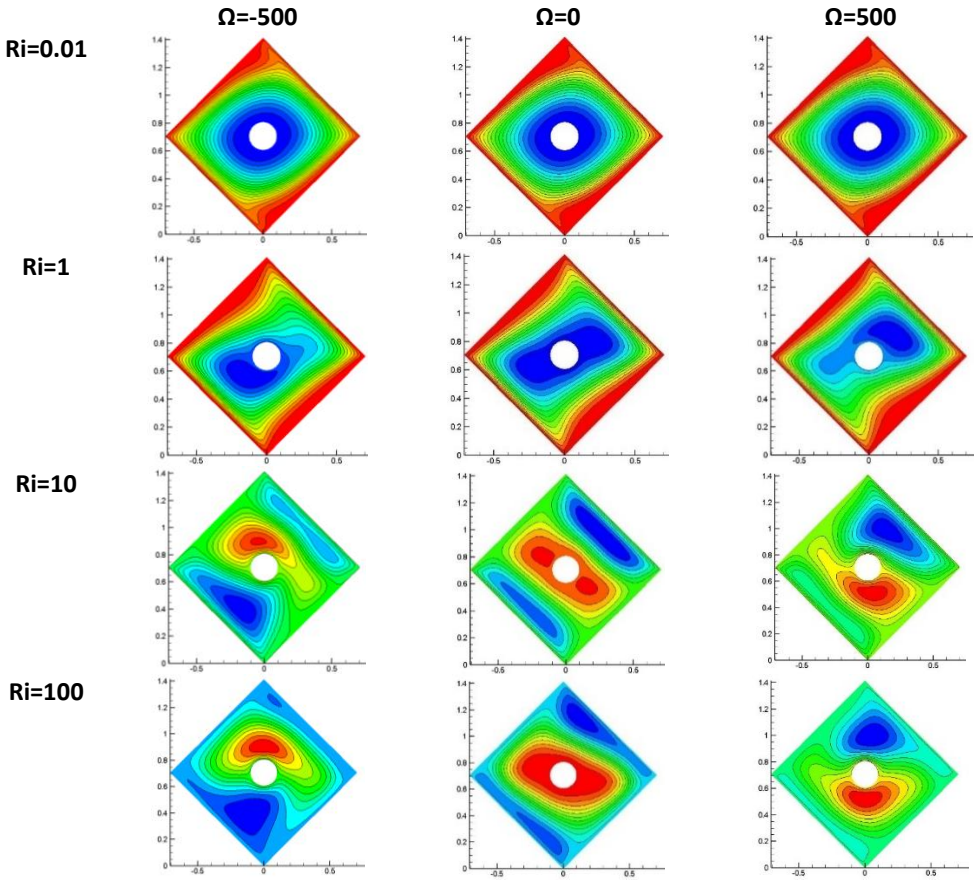

Fig. 11. Streamlines for 0.01 ≤ Ri ≤ 100, -500 ≤ Ω ≤ 500, R = 0.1 and γ=45°

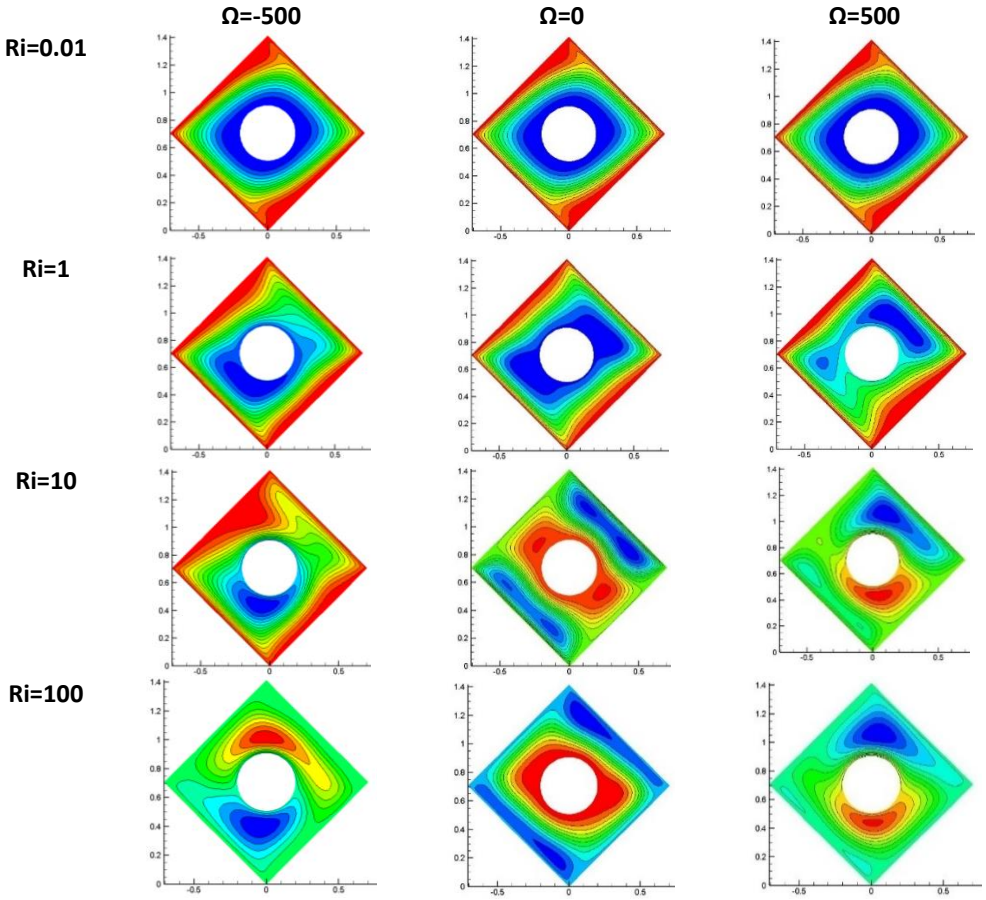

Fig. 12. Streamlines for 0.01 ≤ Ri ≤ 100, -500 ≤ Ω ≤ 500, R = 0.2 and γ=45°

The local Nusselt number along the hot bottom wall for various cylinder angular velocities at Gr=10000, ϕ=0.02, R=(0.1, 0.2), γ= 90°, and Ri= 100 is shown in Figs. 13 and 14. The Nux in Figs. 13 and 14 rises with a counterclockwise angular rotational speed. On the two edges, the curves diverge and are negative. The local Nusselt number Nux = 3.22 maximum value for x = 0.57 corresponds to Ω= -500; after this point, the values decrease. The most significant value of Nux in Fig. 14 is 3.42 when x = 0.57. The Nusselt number rises and the heat transmission rate improve when the cylinder radius and rotational speed increase. The cylinder speed does encourage better fluid circulation in the hollow. Convection transfer is improved by unevenly heating the bottom wall.

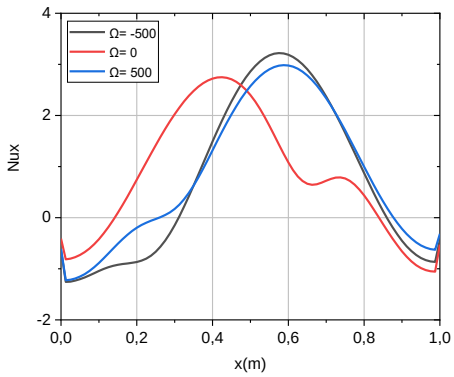

Fig. 13. Local Nusselt number for -500 ≤ Ω ≤500, Gr=10000, ϕ=0.02,γ = 90 °, R= 0.1 and Ri=100

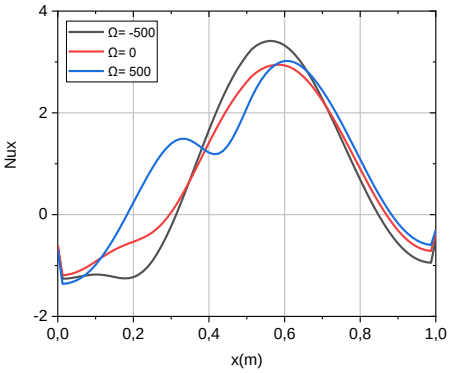

Fig. 14. Local Nusselt number for -500 ≤ Ω ≤ 500,Gr=10000, ϕ=0.02, γ = 90 °, R= 0.2 and Ri=100

The local Nusselt number along the hot bottom wall for different angular velocities of the cylinder at Gr=10000, ϕ=0.02, R=(0.1, 0.2), and γ=45° is shown in Figs. 15 and 16. The most significant value of the local Nusselt number Nux = 3 for x = 0.44 corresponds to Ω= -500 in Fig. 15, after which there is a non-uniform drop along the hot wall. Fig. 16 shows the most significant value of Nux = 3.14 for x = 0.45, indicating a significant thermal performance in this region. The two moving vertical walls and the cylinder's rotational speed significantly impact the convection rate, which is why it is increasing. Local Nusselt numbers, therefore, rise as the cylinder rotational speed increases. The heat transmission rate increases with a 90° inclination angle compared to a 45° angle.

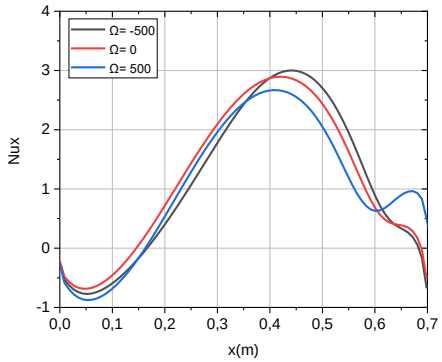

Fig. 15. Local Nusselt number for -500 ≤ Ω ≤ 500, Gr=10000, ϕ=0.02, γ = 45 °, R= 0.1 and Ri=100

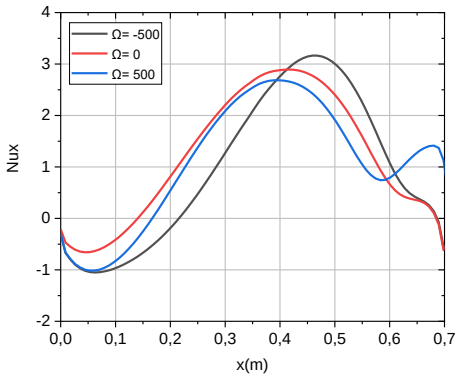

Fig. 16. Local Nusselt number for -500 ≤ Ω ≤ 500, Gr=10000, ϕ=0.02,γ = 45 °, R= 0.2 and Ri=100

The local Nusselt number along the heated bottom wall for different Ri values at Gr=10000, ϕ=0.02, R=(0.1, 0.2), andγ = 45° is shown in Figs. 17 and 18. In the figures, Ri = 0.01 corresponds to the local Nusselt number Nux = 28.35, the maximum value for x = 0.7. As a result, when Richardson numbers are low, there are more local Nusselts. According to Richardson, the number of Nux varies greatly.

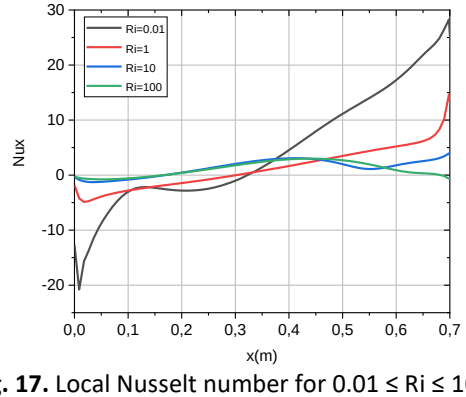

Fig. 17. Local Nusselt number for 0.01 ≤ Ri ≤ 100, Gr=10000, ϕ=0.02 ,γ = 45 ° R= 0.1 and Ω=-500

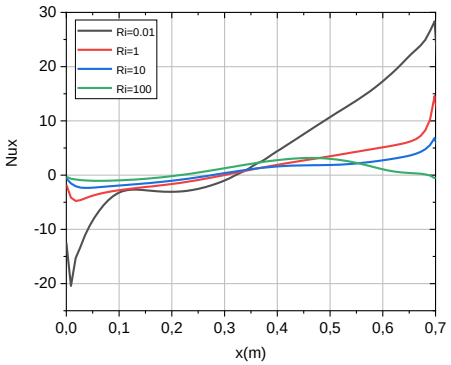

Fig. 18. Local Nusselt number for 0.01 ≤ Ri ≤ 100,Gr=10000, ϕ=0.02 ,γ = 45°, R= 0.2 and Ω=-500

The average Nusselt number for the cylinder along the sinusoidal heated bottom wall for Gr=10000, ϕ=0.02, R=(0.1, 0, 2), and γ= 45° is shown in Figs. 19 and 20. In the figures, the maximum average Nusselt number is Nuavg = 4.5, and the constant for each angular rotational speed is Ri = 0.01. As a result, as the Richardson number rises, the average Nusselt number falls. According to Richardson, there are many variations in the number of Nuavg. The averaged Nusselt number rises as the Richardson number decreases. A heat transfer enhancement of 41% is achieved for Ri = 1 compared to Ri = 10, and 70% for Ri = 0.01 compared to Ri = 1.

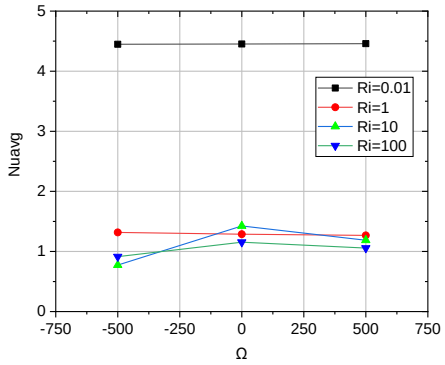

Fig. 19. The average number of Nusselt for Gr=10000, ϕ=0.02, γ = 45° and R= 0.1

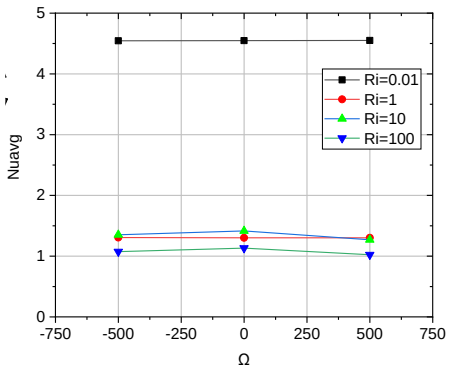

Fig. 20. The average number of Nusselt for Gr=10000, ϕ=0.02,γ = 45° and R= 0.2

5. CONCLUSION

This computational study examines the impact of cylindrical obstacles on convection within an inclined enclosure containing an Al_2O_3-water nanofluid. In-depth research has been done on the effects of the Richardson numbers, rotational speed, and cylinder radius. The key findings are outlined as follows:

- The local and average Nusselt numbers rise when the Richardson number falls. This indicates that the heat transmission coefficient is influenced by convection.
- It was found that heating the lower wall at a sinusoidal temperature rather than a constant temperature enhances heat transmission.
- The cylinder's rotating speed impacts the cavity, increasing fluid heat flow and improving thermal performance through convection.
- A cylinder with a wider radius can be used to achieve a higher heat transmission rate. The ratio of the rate of increase of the Nusselt number of the cylinder along the heated sinusoidal bottom wall is 46%.
- Mixed convection has a great thermal performance since it uses nanofluid.
- The vertical wall shifting improves the effect of the mixed convection flow.

Conflicts of Interest

The authors declare no conflict of interest.

REFERENCES

[1] B. Karbasifar, M. Akbari, D. Toghraie, Mixed convection of Water-Aluminum oxide nanofluid in an inclined lid-driven cavity containing a hot elliptical centric cylinder. *International Journal of Heat and Mass Transfer*, 116, 2018: 1237-1249. https://doi.org/10.1016/j.ijheatmasstransfer.2017.09.110

[2] A.J. Chamkha., E. Abu-Nada, Mixed convection flow in single-and double-lid driven square cavities filled with water–Al_2O_3 nanofluid: Effect of viscosity models. *European Journal of Mechanics-B/Fluids*, 36, 2012: 82-96. https://doi.org/10.1016/j.euromechflu.2012.03.005

[3] F.A. Soomro, R.U. Haq, E.A. Algehyne, I. Tlili, Thermal performance due to magnetohydrodynamics mixed convection flow in a triangular cavity with circular obstacle. *Journal of Energy Storage*, 31, 2020: 101702.

https://doi.org/10.1016/j.est.2020.101702

[4] S.K. Pal, S. Bhattacharyya, I. Pop, A numerical study on non-homogeneous model for the conjugate-mixed convection of a Cu-water nanofluid in an enclosure with thick wavy wall. *Applied Mathematics and Computation*, 356, 2019: 219-234. https://doi.org/10.1016/j.amc.2019.03.008

[5] M. Muthtamilselvan, D.H. Doh, Mixed convection of heat generating nanofluid in a lid-driven cavity with uniform and non-uniform heating of bottom wall. *Applied Mathematical Modelling*, 38(13), 2014: 3164-3174. https://doi.org/10.1016/j.apm.2013.11.033

[6] E. Abu-Nada, Z. Masoud, A. Hijazi, Natural convection heat transfer enhancement in horizontal concentric annuli using nanofluids. *International Communications in Heat and Mass Transfer*, 35(5), 2008: 657-665. https://doi.org/10.1016/j.icheatmasstransfer.2007.11.004

[7] S. Yousefzadeh, H. Rajabi, N. Ghajari, M.M. Sarafraz, O. A. Akbari, M.Goodarzi, Numerical investigation of mixed convection heat transfer behavior of nanofluid in a cavity with different heat transfer areas. *Journal of Thermal Analysis and Calorimetry*, 140, 2020: 2779-2803. https://doi.org/10.1007/s10973-019-09018-6

[8] M. Shekaramiz, S. Fathi, H.A. Ataabadi, H. Kazemi-Varnamkhasti, D. Toghraie, MHD nanofluid free convection inside the wavy triangular cavity considering periodic temperature boundary condition and velocity slip mechanisms. *International Journal of Thermal Sciences*, 170, 2021: 107179. https://doi.org/10.1016/j.ijthermalsci.2021.107179

[9] L.M. Jasim, H. Hamzah, C. Canpolat, B. Sahin, Mixed convection flow of hybrid nanofluid through a vented enclosure with an inner rotating cylinder. *International Communications in Heat and Mass Transfer*, 121, 2021: 105086. https://doi.org/10.1016/j.icheatmasstransfer.2020.105086

[10] W. Al-Kouz, B. A.-I. Bendrer, A. Aissa, A. Almuhtady, W. Jamshed, K.S. Nisar, A. Mourad, N.A. Alshehri, M. Zakarya, Galerkin finite element analysis of magneto two-phase nanofluid flowing in double wavy enclosure comprehending an adiabatic rotating cylinder. *Scientific Reports*, 11, 2021: 16494. https://doi.org/10.1038/s41598-021-95846-2

[11] A.R. Rahmati, A.A. Tahery, Numerical study of nanofluid natural convection in a square cavity with a hot obstacle using lattice Boltzmann method. *Alexandria Engineering Journal*, 57(3), 2018: 1271-1286. https://doi.org/10.1016/j.aej.2017.03.030

[12] S. Sivanandam, A.J. Chamkha, F.O.M. Mallawi, M.S. Alghamdi, A.M. Alqahtani, Effects of entropy generation, thermal radiation and moving-wall direction on mixed convective flow of nanofluid in an enclosure. *Mathematics*, 8(9), 2020: 1471. https://doi.org/10.3390/math8091471

[13] F. Selimefendigil, Mixed convection in a lid-driven cavity filled with single and multiple-walled carbon nanotubes nanofluid having an inner elliptic obstacle. *Propulsion and Power Research*, 8(2), 2019: 128-137. https://doi.org/10.1016/j.jppr.2019.01.007

[14] F.M. Azizul, A.I. Alsabery, I. Hashim, Heatlines visualisation of mixed convection flow in a wavy heated cavity filled with nanofluids and having an inner solid block. *International Journal of Mechanical Sciences*, 175, 2020: 105529. https://doi.org/10.1016/j.ijmecsci.2020.105529

[15] S.E.B. Maiga, S.J. Palm, C.T. Nguyen, G. Roy, N. Galanis, Heat transfer enhancement by using nanofluids in forced convection flows. *International Journal of Heat and Fluid Flow*, 26(4), 2005: 530-546. https://doi.org/10.1016/j.ijheatfluidflow.2005.02.004

[16] V. Ambethkar D. Kushawaha, Numerical simulations of fluid flow and heat transfer in a four-sided, lid-driven rectangular domain. *International Journal of Heat and Technology*, 35, 2017: 1-10. https://doi.org/10.48550/arXiv.1705.00707

[17] M.T. Al-Asadi, H.A. Mohammed, A.S. Kherbeet, A.A. Al-Aswadi, Numerical study of assisting and opposing mixed convective nanofluid flows in an inclined circular pipe. *International Communications in Heat and Mass Transfer*, 85, 2017: 81-91. https://doi.org/10.1016/j.icheatmasstransfer.2017.04.015

[18] M.S.M. Saleh, S. Mekroussi, S. Kherris, D. Zebbar, N. Belghar, A numerical investigation of the effect of sinusoidal temperature on mixed convection flow in a cavity filled with a nanofluid with moving vertical walls. *Heat Transfer*, 52(1), 2023: 7-27. https://doi.org/10.1002/htj.22683

[19] B. Abbou, S. Mekroussi, H. Ameur, S. Kherris, Effect of aspect ratio and nonuniform temperature on mixed convection in a double lid-driven cavity. *Numerical Heat Transfer, Part A: Applications*, 83(3), 2023: 237-247. https://doi.org/10.1080/10407782.2022.2091365

[20] L. Saidi, S. Mekroussi, S. Kherris, D. Zebbar, B. Mébarki, A Numerical Investigation of the Free Flow in a Square Porous Cavity with Non-Uniform Heating on the Lower Wall. *Engineering, Technology & Applied Science Research,* 12(1), 2022: 7982-7987. https://doi.org/10.48084/etasr.4604

[21] A.I. Alsabery, E. Gedik, A.J. Chamkha, I. Hashim, Impacts of heated rotating inner cylinder and two-phase nanofluid model on entropy generation and mixed convection in a square cavity. *Heat and Mass Transfer*, 56, 2020: 321-338. https://doi.org/10.1007/s00231-019-02698-8

[22] A.A.A. Arani, J. Amani, M. Hemmat Esfeh, Numerical simulation of mixed convection flows in a square double lid-driven cavity partially heated using nanofluid. *Journal of Nanostructures*, 2(3), 2012: 301-311. https://doi.org/10.7508/jns.2012.03.005

[23] S.Y. Ahmed, M.Y. Jabbar, H.K. Hamzah, F.H. Ali, A. K. Hussein, Mixed convection of nanofluid in a square enclosure with a hot bottom wall and a conductive half-immersed rotating circular cylinder. *Heat Transfer*, 49(8), 2020: 4173-4203. https://doi.org/10.1002/htj.21822

[24] Z. Li, P. Barnoon, D. Toghraie, R.B. Dehkordi, M. Afrand, Mixed convection of non-Newtonian nanofluid in an H-shaped cavity with cooler and heater cylinders filled by a porous material: Two phase approach. *Advanced Powder Technology*, 30(11), 2019: 2666-2685. https://doi.org/10.1016/j.apt.2019.08.014

[25] M.H. Esfe, M. Akbari, D.S. Toghraie, A. Karimipour, M. Afrand, Effect of nanofluid variable properties on mixed convection flow and heat transfer in an inclined two-sided lid-driven cavity with sinusoidal heating on sidewalls. *Heat Transfer Research*, 45(5), 2014: 409-432. https://doi.org/10.1615/HeatTransRes.2013007127

[26] A.A.A. Arani, S.M. Sebdani, M. Mahmoodi, A. Ardeshiri, M. Aliakbari, Numerical study of mixed convection flow in a lid-driven cavity with sinusoidal heating on sidewalls using nanofluid. *Superlattices and Microstructures*, 51(6), 2012: 893-911. https://doi.org/10.1016/j.spmi.2012.02.015

[27] H.C. Brinkman, The Viscosity of Concentrated Suspensions and Solutions. *The Journal of Chemical Physics*, 20(4), 1952: 571-571. https://doi.org/10.1063/1.1700493

[28] N.S. Nagulkar, S.M. Lawankar, Improving the Cooling Performance of Automobile Radiator with Ethylene Glycol Water Based ZrO_2 Nanofluid and Compare with Al_2O_3 Nanofluid. *International Research Journal of Engineering and Technology (IRJET)*, 4(7), 2017: 1255-1260.

[29] S. Patankar, Numerical Heat Transfer and Fluid Flow. *Boca Raton: CRC Press*, 2018.

[30] M.K. Moallemi, K.S. Jang, Prandtl number effects on laminar mixed convection heat transfer in a lid-driven cavity. *International Journal of Heat and Mass Transfer*, 35(8), 1992: 1881-1892. https://doi.org/10.1016/0017-9310(92)90191-T

[31] M.A. Waheed, Mixed convective heat transfer in rectangular enclosures driven by a continuously moving horizontal plate. *International Journal of Heat and Mass Transfer*, 52(21-22), 2009: 5055-5063. https://doi.org/10.1016/j.ijheatmasstransfer.2009.05.011

[32] R.K. Tiwari, M.K. Das, Heat transfer augmentation in a two-sided lid-driven differentially heated square cavity utilizing nanofluids. *International Journal of Heat and Mass Transfer*, 50(9-10), 2007: 2002-2018. https://doi.org/10.1016/j.ijheatmasstransfer.2006.09.034

[33] M.M. Abdelkhalek, Mixed convection in a square cavity by a perturbation technique. *Computational Materials Science*, 42(2), 2008: 212-219. https://doi.org/10.1016/J.COMMATSCI.2007.07.004

[34] K.M. Khanafer, A.J. Chamkha, Mixed convection flow in a lid-driven enclosure filled with a fluid-saturated porous medium. *International Journal of Heat and Mass Transfer*, 42(13), 1999: 2465-2481. https://doi.org/10.1016/S0017-9310(98)00227-0

[35] M.R. Sharif, Laminar mixed convection in shallow inclined driven cavities with hot moving lid on top and cooled from bottom. *Applied Thermal Engineering*, 27(5-6), 2007: 1036-1042. https://doi.org/10.1016/j.applthermaleng.2006.07.035

[36] K.M. Khanafer, A.M. Al-Amiri, I. Pop, Numerical simulation of unsteady mixed convection in a driven cavity using an externally excited sliding lid. *European Journal of Mechanics-B/Fluids*, 26(5), 2007: 669-687. https://doi.org/10.1016/j.euromechflu.2006.06.006